

# $^{31}\text{P}$ and $^{27}\text{Al}$ Solid-State Nuclear Magnetic Resonance Study of Taranakite

William F. Bleam<sup>1</sup>, Philip E. Pfeffer<sup>1</sup>, and James S. Frye<sup>2</sup>

**Abstract.** High-resolution  $^{27}\text{Al}$  solid-state nuclear magnetic resonance (NMR) spectroscopy indicates that aluminum in taranakite is probably restricted to six-coordinate sites. High-resolution  $^{31}\text{P}$  solid-state NMR spectroscopy reveals that phosphate groups exist in two environments in taranakite. The rate of  $^1\text{H}$ -induced dipolar dephasing of the  $^{31}\text{P}$  signals in cross-polarization, magic-angle-spinning NMR spectra of taranakite suggests that one or more oxygens of one of two phosphates are directly protonated. The same experiments suggests that the oxygens of the second form of phosphate are not directly protonated but may be hydrogen-bond receptors. The ratio of protonated phosphate to non-protonated phosphate, as measured from  $^{31}\text{P}$  single-pulse excitation, magic-angle-spinning spectra, is approximately one to three.

## Introduction

### *Taranakite Structural Studies*

The structure of taranakite is unknown; no crystal suitable for single-crystal structure determination and refinement has ever been obtained. Taranakite's platy crystal-habit lead Smith and Brown (1959) to suggest that it probably has a layered structure. Their proposed formula for the potassium-rich phase (viz.,  $\text{H}_6\text{K}_3\text{Al}_3(\text{PO}_4)_8 \cdot n\text{H}_2\text{O}$ ;  $n = 13, 18$ ) is the one most commonly cited in the literature. In the absence of a crystal structure refinement, of course, this cannot be confirmed or disproved. Sakae and Sudo (1975) described a naturally occurring taranakite from the Onino-Iwaya limestone cave, Japan with the empirical formula:  $\text{H}_{7.09}\text{K}_{1.97}(\text{Al}, \text{Fe})_{4.98}(\text{PO}_4)_8 \cdot 19.7\text{H}_2\text{O}$ . Protons substituting for potassium ions, according to their explanation, could account for the compositional difference between the Onino-Iwaya taranakite and the synthetic taranakite described by Smith and Brown (1959).

Boldog et al. (1979) were the first to suggest that acidic phosphate groups exist in taranakite. They assigned several infrared bands to P-O-H bending and PO-H stretching vibrations of acid phosphates. Based on  $^1\text{H}$  nuclear magnetic resonance (NMR) spectra, Boldog et al. (1979) concluded

that the most likely form of acid phosphate in taranakite was the  $\text{H}_2\text{PO}_4$ -anion.

By proposing a structure analogous to illite, McConnell (1976) assigned an alternative role to taranakite protons. In McConnell's (1976) hypothetical phyllophosphate, some of the protons presumably substitute for phosphorus in 4-coordinate sites, others for aluminum in 6-coordinate sites. McConnell (1976) also has aluminum occupying both 4-coordinate and 6-coordinate sites.

Moore and Araki (1979) suspect the structure of a synthetic crystalline ammonium iron phosphate, named "Product K", is structurally similar to taranakite. "Product K",  $(\text{NH}_4)_2\text{H}_8\text{Fe}_3(\text{PO}_4)_6 \cdot 6\text{H}_2\text{O}$ , contains two crystallographically distinct orthophosphates. One of these phosphates is the doubly-protonated  $\text{H}_2\text{PO}_4$ -anion. The two protons associated with the second type of phosphate, based on computed electrostatic bond strengths, are bonded to two symmetrically independent oxygen atoms. The ratio of the protonated to non-protonated phosphate is 1:1. All of the iron in "Product K" is 6-fold coordinated.

The preceding discussion focuses attention on both the structural role of taranakite protons and aluminum coordination. Questions of this sort may yield to measurements made with high-resolution solid-state NMR spectroscopy (Andrew 1981; Fyfe et al. 1982, 1983; Kirkpatrick et al. 1985; Nagy et al. 1985; Oldfield and Kirkpatrick 1985).

### *Aluminum-27 Solid-state NMR*

$^{27}\text{Al}$  isotropic chemical-shifts have been used to distinguish between 4-, 5- and 6-fold aluminum coordination environments (Müller et al. 1981; Lippmaa et al. 1986; Mastikhin and Zamaraev 1987), yet it is clear that the interpretation of NMR spectra from half-integer quadrupolar nuclei such as  $^{27}\text{Al}$  ( $I = 5/2$ ) is not a simple exercise and must be approached with care. Early NMR studies revealed that often a substantial portion of the aluminum known to be present in the sample, whether solution (Akitt and Farthing 1978) or solid (Resing and Rubinstein 1978), was not observable.

Besides dipole-dipole interactions and chemical-shift anisotropy, the central transition ( $m = 1/2 \leftrightarrow m = 1/2$ ) of half-integer quadrupolar nuclei is subject to broadening caused by the interaction between the nuclear quadrupolar moment and the electric-field gradient at the nucleus. The latter is believed to be the primary cause of  $^{27}\text{Al}$  signal loss (Bosacek et al. 1982) although significant broadening also occurs in samples with transition-metal contents greater than 1%

*Current address:* Department of Soil Science, 1525 Observatory Drive, University of Wisconsin-Madison, Madison, WI 53706, USA

(Oldfield et al. 1983; Sanz and Serratos 1984). Signal loss in certain cases can be as high as 95% (De Jong et al. 1983; MacKenzie et al. 1985).

Coherence between the central and satellite transitions develops during the initial, on-resonance excitation pulse (i.e., the "preparation" step) used in every Fourier-Transform NMR experiment. Signal intensity is influenced, in part, by this coherence. The rate at which it develops, for a given specie, depends on its quadrupolar coupling constant (Samoson and Lippmaa 1983; Fenzke et al. 1984). As coherence develops and satellite transitions are excited, the transverse magnetization oscillates at the frequency of the radio-frequency field,  $\omega_{rf}$ .

For a pulse length  $\tau_p \leq \pi/4\omega_{rf}(I+1/2)$ , intensity is proportional to  $\tau$  and independent of the quadrupolar-coupling constant. If  $\tau_p > \pi/4\omega_{rf}(I+1/2)$ , the central-transition intensity will be greater for those nuclei with smaller quadrupolar-coupling constants. As an example, if the sample contains aluminum ( $I=5/2$ ) in a chemical environment characterized by a quadrupolar coupling constant greater than, say, 1 MHz and the excitation pulse is  $\pi/3\omega_{rf}$ , the signal will be totally eliminated (Fenzke et al. 1984). For  $^{27}\text{Al}$ , one must chose an excitation pulse length of less than or equal to  $\pi/12\omega_{rf}$  to avoid the effect of quadrupolar-coupling constants on signal intensity.

Differential loss of signal intensity can also occur because of the finite recovery time for the receiver following the excitation pulse. The initial portion of the transverse magnetization free-induction decay (FID) is the most critical part for broad-line signals. Loss of this initial portion of the FID results in an underestimate of broad-line signal intensities (Müller et al. 1983a).

The quadrupolar coupling constants for aluminum in 4-fold coordination are generally less than for 6-coordinate sites (Müller et al. 1981; Akitt and Farthing 1978; Lampe et al. 1982; Stade et al. 1984). Müller et al. (1983a) believe this is because 6-coordinate aluminum polyhedra are easier to distort than 4-coordinate polyhedra, Al-O bond lengths being greater (and the bond strengths lower) in the former than in the latter.

The results from minerals containing 5-coordinate aluminum (Cruikshank et al. 1986; Alemany and Kirker 1986; Lippmaa et al. 1986; Gilson et al. 1987; Risbud et al. 1987; Alemany et al. 1988) illustrate the final issue we will consider concerning  $^{27}\text{Al}$  NMR. Intuitively, one would expect 5-coordinate polyhedra to be more extreme distortions from cubic symmetry than 4- or 6-coordinate polyhedra, yet  $^{27}\text{Al}$  spectra of 5-coordinate aluminum are readily observed in those crystalline compounds studied to date. Loss of  $^{27}\text{Al}$  signal intensity is more common in amorphous or poorly crystalline materials (Resing and Rubinstein 1978; Bosacek et al. 1982; Klinowski et al. 1982) than crystalline compounds (De Jong et al. 1983; Engelhardt et al. 1983).

Short of direct spin-counting, an experiment fraught with difficulty (Kirkpatrick et al. 1986), one can never be certain whether all of the  $^{27}\text{Al}$  intensity is observed. However, if one takes precautions to use short excitation pulses and to acquire the initial portion of the FID, one may observe most of the  $^{27}\text{Al}$  signal even in amorphous materials (Cheung et al. 1986; Oestrike et al. 1987). The expectation of observing all 6- or 5-fold coordinate aluminum should be greater in crystalline compounds than amorphous materials.

### Phosphorus-31 Solid-state NMR

We now turn to a discussion of NMR techniques probing the structural role of protons. One strategy for measuring  $^1\text{H}$ - $^{31}\text{P}$  nuclear magnetic dipole interactions uses variations of the cross-polarization (CP) experiment of Pines et al. (1973). For instance, Rothwell et al. (1980) and Tropp et al. (1983) made qualitative comparisons of CP, magic-angle-spinning (CP-MAS) and single-pulse excitation, magic-angle-spinning (MAS) spectra. The  $^{31}\text{P}$  resonances more strongly coupled to  $^1\text{H}$  show a relative enhancement in the CP-MAS spectra when compared to MAS spectra.

Aue and co-workers (Aue et al. 1984; Roufosse et al. 1984) extended this strategy by including "dipolar suppression", also known as "interrupted-decoupling" (Opella and Frey 1979) CP-MAS experiments. The  $^{31}\text{P}$  resonances more strongly coupled to  $^1\text{H}$  show a relative suppression in the interrupted-decoupling CP-MAS spectra when compared to MAS spectra. Others (Maciel and Sindorf 1980; Grimmer et al. 1986) have quantified heteronuclear nuclear-magnetic-dipole interactions by measuring the cross-polarization-relaxation time,  $T_{\text{PH}}$ .

### Experimental Methods and Materials

Proton-decoupled  $^{31}\text{P}$  spectra were obtained on three different spectrometers: 1) a modified Nicolet NT-150 NMR spectrometer operating at 3.5 T,  $^{31}\text{P}$  frequency = 60.745 MHz; 2) a Bruker CXP-200 spectrometer at 4.67 T,  $^{31}\text{P}$  frequency = 80.98 MHz; and 3) a JEOL FX60QS spectrometer at 1.4 T,  $^{31}\text{P}$  frequency = 24.15 MHz. The  $90^\circ$  pulse width for the NT-150 spectrometer was 6  $\mu\text{s}$  for both  $^1\text{H}$  and  $^{31}\text{P}$ , decoupling time was 52 ms, contact time was 2 ms and spinning frequencies were approximately 3.5 kHz. On the CXP-200 spectrometer the  $90^\circ$  pulse was 6.5  $\mu\text{s}$  for  $^1\text{H}$  with a decoupling field of 0.91 mT, a contact time of 1.5 ms and spinning frequencies of approximately 8 kHz. Finally, the  $90^\circ$  pulse was 6.3  $\mu\text{s}$  on the FX60QS spectrometer, the contact time for maximum signal intensity was 0.7 ms, the  $^1\text{H}$  decoupling field was 0.91 mT and the spinning frequencies were approximately 2 kHz. "Interrupted-decoupling" (also known as "dipolar-dephasing") CP-MAS experiments were performed by inserting a variable delay time *without*  $^1\text{H}$  decoupling following the contact time and before acquisition of the free-induction decay. These delay times without proton decoupling ranged from 10  $\mu\text{s}$  to 250  $\mu\text{s}$ .

$^{27}\text{Al}$  spectra were collected on a Bruker AM-500 spectrometer with "home-built" magic-angle-spinning probe operating at 11.75 T,  $^{27}\text{Al}$  frequency = 130.32 MHz. A  $\pi/2$  pulse is 16  $\mu\text{s}$ , but our spectra were accumulated with only a 1  $\mu\text{s}$  pulse. The spinning frequencies on the order of 13 kHz were attained using a Torlon rotor. Line broadening was 200 Hz and delay times between acquisitions were evaluated at both 0.004 ms and 250 ms to verify that  $T_{1\text{Al}}$  relaxation was not affecting relative signal intensities.

We used two taranakites in our study (Table 1). The naturally-occurring taranakite (NMNH # R5530: Grotte de Minerve, Hérault, France) was provided by the Department of Mineral Sciences, National Museum of Natural History, Smithsonian Institution, Washington, DC. The synthetic taranakite was prepared according to the technique of Taylor and Gurney (1961). X-ray powder diffraction of the

**Table 1.** Aluminum phosphate minerals used in this study

Mineral	Identification	Formula	Space group
Variscite	NMNH # 87484-5	$\text{AlPO}_4 \cdot 2\text{H}_2\text{O}$	<i>Pbca</i>
Wavellite	NMNH # R16042	$\text{Al}_3(\text{OH})_3(\text{PO}_4)_2 \cdot 5\text{H}_2\text{O}$	<i>Pcmm</i>
Crandallite	NMNH # 104085-2	$\text{CaAl}_3(\text{OH})_6(\text{PO}_4)_3$	<i>R\bar{3}m</i>
Monetite	synthetic <sup>a</sup>	$\text{CaHPO}_4$	<i>P\bar{1}</i>
Potassium dihydrogen phosphate	synthetic <sup>a</sup>	$\text{KH}_2\text{PO}_4$	<i>I42d</i>
Taranakite	NMNH # R5530	$\text{H}_6\text{K}_3\text{Al}_5(\text{PO}_4)_8 \cdot 18\text{H}_2\text{O}$	b
Taranakite	synthetic	$\text{H}_6\text{K}_3\text{Al}_5(\text{PO}_4)_8 \cdot 13\text{H}_2\text{O}$	b

<sup>a</sup> Fisher Scientific, Certified Reagent

<sup>b</sup> *R3c* or *R\bar{3}c*, Smith and Brown (1959)

two taranakites was performed on a Philips X-ray diffractometer (Co  $K_\alpha$  radiation, 30 kV, 10 mA).

We also include NMR data for crandallite (NMNH # 104085-2: Fairfield, Utah), variscite (NMNH # 87484-5: Lucin, Utah), and wavellite (NMNH # R16042: Montgomery, Arkansas); supplied by the Department of Mineral Sciences, National Museum of Natural History, Smithsonian Institution, Washington, DC. The potassium and calcium phosphates,  $\text{KH}_2\text{PO}_4$  and  $\text{CaPO}_4$ , were Certified Reagents from Fisher Scientific Co.

## Experimental Results

### Powder X-ray Diffraction

The most prominent x-ray powder diffraction lines from the Grotte de Minerve taranakite are: 15.6 Å (100), 7.47 Å (36), 3.82 Å (60) and 3.14 Å (54). These diffraction lines compare quite well with published powder x-ray data (Haseman et al. 1950; Sakae and Sudo 1975; Boldog et al. 1979; Nriagu 1984) and with data listed in Card # 29-981 of the *X-ray Powder Diffraction File* (PDF) maintained by the International Center for Diffraction Data.

The synthetic taranakite yields a different set of x-ray powder diffraction lines: 13.8 Å (100), 7.37 Å (36), 6.88 Å (44) and 3.40 Å (44). At first it may appear that the synthetic sample is not a taranakite; however, there are several published accounts of "lower hydrates" of taranakite with diffraction lines matching the lines recorded for our sample rather closely (Haseman et al. 1950; Smith and Brown 1959; Liu et al. 1966; Sakae and Sudo 1975). These "lower hydrates" are most commonly prepared by heating a taranakite, characterized by the diffraction lines similar to those appearing on PDF Card # 29-981, to temperatures exceeding 95–110° C.

### Aluminum-27 Solid-state NMR

The MAS  $^{27}\text{Al}$  NMR spectrum of the Grotte de Minerve taranakite appears in Fig. 1. A single resonance, its center-of-gravity at  $-8.9$  ppm, dominates the spectrum. The chemical shift corrected for quadrupolar-induced shift (Freude et al. 1985) is  $-3.0$  ppm. We obtained our  $^{27}\text{Al}$  spectra of the Grotte de Minerve taranakite with a spectral width of 125 kHz. No very broad signals were evident at large vertical expansion, so the spectrum provides no evidence for aluminum sites with unusually large quadrupolar-coupling-constants. We would expect a much lower signal-

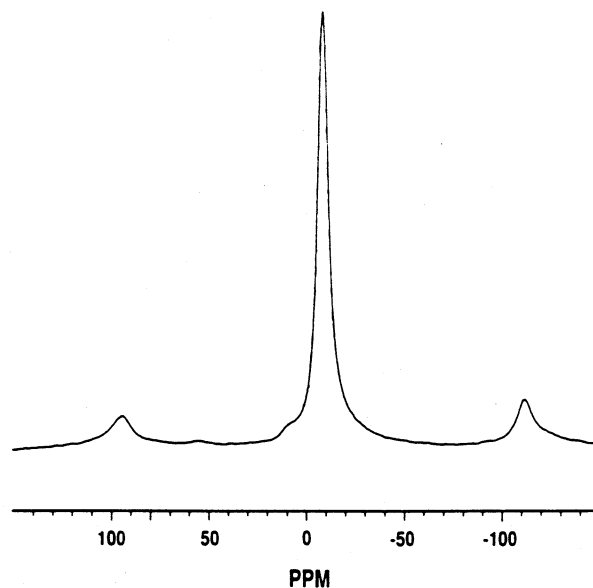


**Fig. 1.** 130.32 MHz  $^{27}\text{Al}$  solid-state NMR spectra with 1 M  $\text{AlCl}_3$  (aq) used as an external chemical shift reference. Natural taranakite [NMNH # R5530] single-pulse excitation, MAS at 13.4 kHz spinning frequency: 50000 scans, 1k data points, 125 kHz spectral width, 4 ms delay between pulses

to-noise ratio for the spectrum in Fig. 1 if a major proportion of the aluminum were present in low-symmetry coordination sites and, hence, not observed.

Delays as long as 250 ms between pulses tested the possibility that resonances with rotating-frame longitudinal-relaxation times,  $T_{1\rho\text{Al}}$ , longer than the  $T_{1\rho\text{Al}}$  of the  $-8.9$  ppm resonance may be present. If there were aluminum nuclei present in the taranakite with long  $T_{1\rho\text{Al}}$ 's they could be saturated with a 0.004 ms delay between pulses and the resonance would not appear in the spectrum. No such resonances appeared in spectra with 250 ms delays between pulses.

### Phosphorus-31 Solid-state NMR

CP-MAS and MAS  $^{31}\text{P}$  NMR spectra from both the Grotte de Minerve and synthetic taranakites appear in Fig. 2. Four resonances at 4.5,  $-0.2$ ,  $-9.2$ , and  $-18.0$  ppm are found in the MAS spectrum of synthetic taranakite (Fig. 2d). The narrow  $-0.2$  ppm resonance is absent from the CP-MAS spectrum (Fig. 2c) and both spectra of the Grotte de

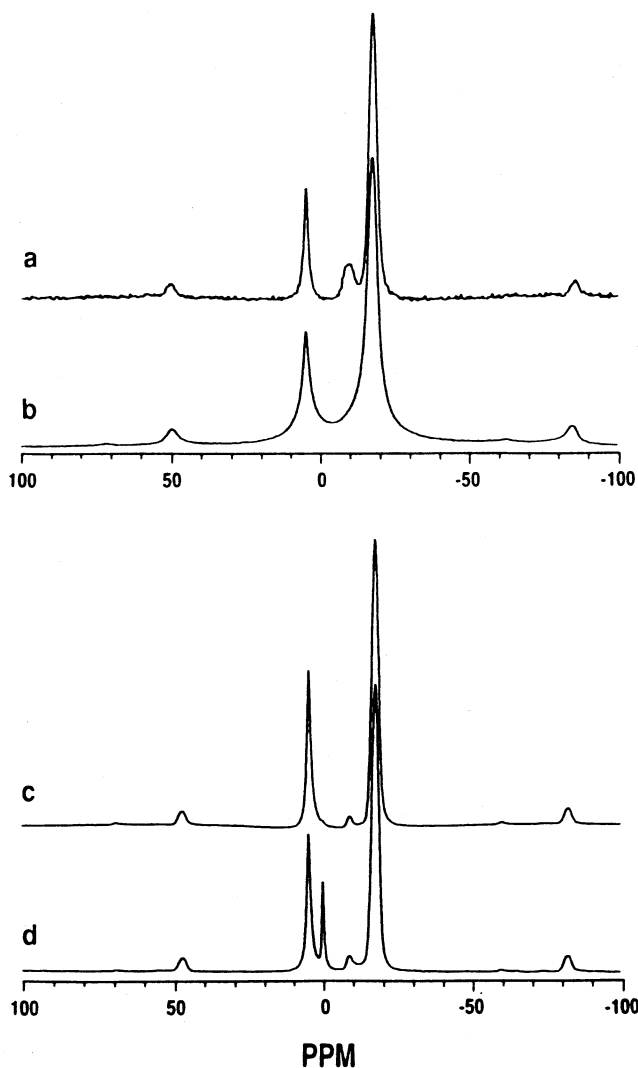


**Fig. 2a–d.** 60.754 MHz  $^{31}\text{P}$  solid-state NMR spectra (85%  $\text{H}_3\text{PO}_4$  external reference): **a** natural taranakite [NMNH # R5530] cross-polarization, MAS with high-power,  $^{31}\text{P}$ - $^1\text{H}$  decoupling: 1000 scans, 4k data points, 20 kHz spectral width, 2 s recycle time, 1 ms contact time; **b** natural taranakite [NMNH # R5530] single-pulse excitation, MAS with high-power,  $^{31}\text{P}$ - $^1\text{H}$  decoupling: 1000 scans, 4k data points, 20 kHz spectral width, 2 s recycle time; **c** synthetic taranakite cross-polarization, MAS with high-power,  $^{31}\text{P}$ - $^1\text{H}$  decoupling: 64 scans, 4k data points, 20 kHz spectral width, 2 s recycle time, 1 ms contact time; and **d** synthetic taranakite single-pulse excitation, MAS with high-power,  $^{31}\text{P}$ - $^1\text{H}$  decoupling: 64 scans, 4k data points, 20 kHz spectral width, 2 s recycle time

Minerve taranakite (Figs. 2a and 2b). One might suppose it identifies the phosphate with weakest  $^1\text{H}$ - $^{31}\text{P}$  interaction since it does not cross polarize. Its absence from the Grotte de Minerve sample indicates that it is an impurity.

Resonances similar to the  $-0.2$  ppm signal have been observed in other synthetic phosphates and has been attributed to a  $\text{H}_3\text{PO}_4$  impurity (J.P. Yesinowski, personal communication). The chemical shift is consistent with this assignment. The absence of cross polarization implies either that there is no static component of the  $^1\text{H}$ - $^{31}\text{P}$  dipolar coupling or that the dipolar coupling, expressed in frequency units, is much weaker than the spinning frequency. A  $\text{H}_3\text{PO}_4$  molecule rapidly tumbling about all axes in a

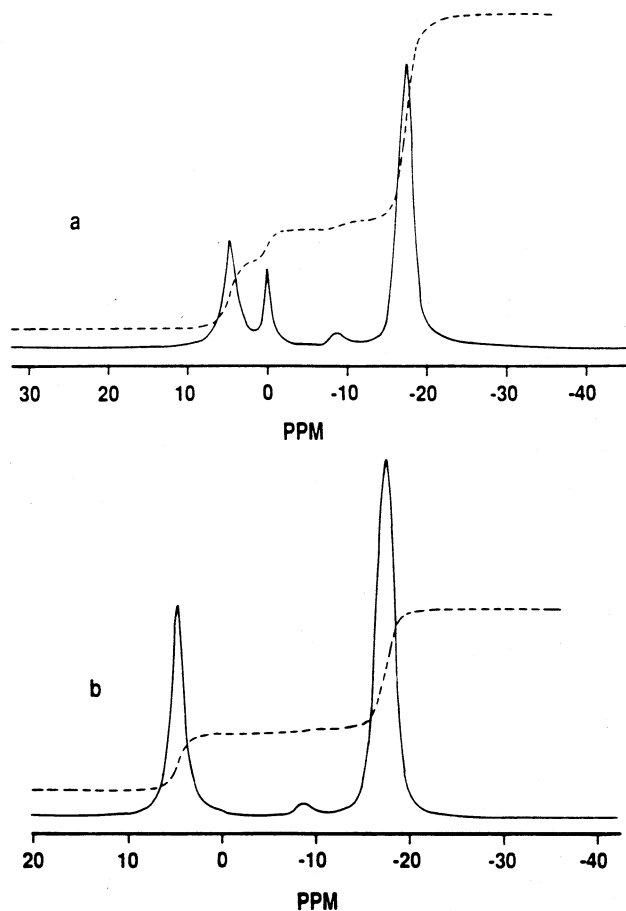


**Fig. 3a, b.** Peak integration for synthetic taranakite resonances. 80.89 MHz  $^{31}\text{P}$  solid-state NMR spectra (85%  $\text{H}_3\text{PO}_4$  external reference): **a** single-pulse excitation, MAS with high-power,  $^{31}\text{P}$ - $^1\text{H}$  decoupling: 50 scans, 8k data points, 20 kHz spectral width, 60 s recycle time; and **b** cross-polarization, MAS with high-power,  $^{31}\text{P}$ - $^1\text{H}$  decoupling: 100 scans, 8k data points, 20 kHz spectral width, 5 s recycle time, 1.5 ms contact time

large pore with few protons on the pore walls could fulfill this condition.

The weak resonance at  $-9.2$  ppm in the CP-MAS spectrum of both Grotte de Minerve and synthetic taranakite is most likely an impurity phase. X-ray powder diffraction gives no evidence of any phases other than taranakite in these samples. If the  $-9.2$  ppm resonance were, in fact; due to a phosphorus environment in taranakite one would be forced to conceive of a structure with two major sites and a small proportion of a third site. In light of the unit cell size and composition and space group symmetry, to be discussed in detail below, we can rule out this possibility and conclude that the  $-9.2$  ppm resonance is an impurity.

Presently, we are at a loss to explain why there is a lower signal-to-noise level in spectrum 2a relative to 2b. It would appear that cross polarization from the proton population is less efficient than direct  $^{31}\text{P}$  pulsing, viz. single-pulse excitation, to generate a  $^{31}\text{P}$  spectrum. A lower signal-to-noise ratio in the CP-MAS experiment (Fig. 2c) relative to the single-pulse excitation (Fig. 2d) is not observed for the synthetic taranakite.  $T_{1\rho\text{H}}$  is likely to be longer than  $T_{1\rho\text{P}}$ , so the relative efficiency of cross polarization probably arises from a long  $T_{\text{PH}}$  or a short  $T_{1\rho\text{H}}$ .

Figure 3 shows the integrated peak areas for the reso-

nances in the synthetic sample. The ratios between the 4.5 ppm and the  $-18.0$  ppm resonances are  $\approx 1:3$  and  $\approx 1:2$  for the MAS experiment (Fig. 3a) and CP-MAS experiment (Fig. 3b), respectively. A contact-time of 1.5 ms was used for the CP experiment appearing in Fig. 3b. MAS spectra yield an estimate of  $\approx 1:2$  as the ratio between the 4.5 ppm resonance and the  $-18$  ppm resonance for the Grotte de Minerve taranakite.

The ratios appearing in Fig. 3 reveal an important difference between phosphorus environments identified by the 4.5 and  $-18.0$  ppm resonances. Tropp et al. (1983) and Aue et al. (1984) convincingly demonstrate that the peak intensities from those nuclei more strongly coupled to protons will be relatively enhanced in CP magic-angle-spinning compared to single-pulse excitation spectra. Clearly, the 4.5 ppm resonance is enhanced relative to the  $-18.0$  ppm resonance when the CP-MAS spectra (Fig. 3b) is compared with the MAS spectra (Fig. 3a). We can conclude that the 4.5 ppm resonance is "more strongly coupled" to the protons in the taranakite than the  $-18.0$  ppm resonance.

As we mentioned above, the structural role of protons in taranakite has been the subject of speculation (Sakae and Sudo 1975; McConnell 1976; Boldog et al. 1979; Moore and Araki 1979). We will examine results from "interrupted-decoupling" experiments designed to yield information about these protons using  $^1\text{H}$ - $^{31}\text{P}$  nuclear magnetic dipole interactions.

We surveyed  $^1\text{H}$ - $^{31}\text{P}$  dipolar dephasing dynamics in a series of well-characterized phosphate structures, including cases with and without phosphate protonation. Dipolar dephasing of  $^{31}\text{P}$  by  $^1\text{H}$  results in a loss of greater than 80% of the  $^{31}\text{P}$  magnetization after 250  $\mu\text{s}$  for all of the minerals illustrated in Fig. 4. Interrupt intervals lasting 500 to 1000  $\mu\text{s}$ , as used by Aue et al. (1984) and Roufosse et al. (1984), would have been too long to distinguish the two resonances in taranakite because both resonances would have been completely de-phased by the time FID acquisition commenced. Short-range interactions dominate the first 100  $\mu\text{s}$  and interrupts on the order of this duration should be used if one wishes to use the potential of this type of experiment.

The curves appearing in Fig. 4 fall in two groups. The magnetization-decay curves for potassium dihydrogen phosphate and the 4.5 ppm resonance of taranakite show

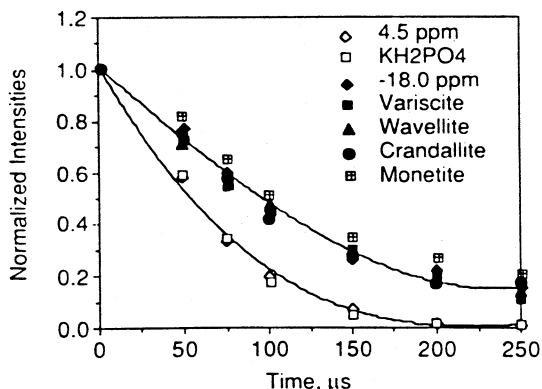


Fig. 4. Signal height as a function of  $^{31}\text{P}$ - $^1\text{H}$  decoupler interrupt time: 24.15 MHz  $^{31}\text{P}$  solid-state NMR spectra; 128 scans, 4k data points, 16 kHz spectral width, 0.7 ms contact time, 2 s recycle time. "4.5 ppm" and " $-18.0$  ppm" refer to signals in the spectrum of natural taranakite

that dephasing is complete after 250  $\mu\text{s}$ . The curves for crandallite, monettite, variscite, wavellite and the  $-18.0$  ppm resonance of taranakite show that about 20% of the magnetization still exists after interrupts lasting 250  $\mu\text{s}$ . In fact, the magnetization-decay curves form two statistically distinct groups.

## Discussion

Not all  $^{27}\text{Al}$  chemical shifts appearing in the literature have been corrected for quadrupolar-induced shifts (Freude et al. 1985; Lippmaa et al. 1986). The corrected  $^{27}\text{Al}$  chemical shift of the Grotte de Minerve taranakite ( $-3.0$  ppm) can be compared to the resonances observed in the  $^{27}\text{Al}$  NMR spectra of  $\text{AlPO}_4$  polymorphs, the aluminophosphate zeolite  $\text{AlPO}_4\text{-5}$ , and calcium aluminum phosphate glasses (Müller et al. 1983a, 1983b; Blackwell and Patton 1984; Müller et al. 1985; Nakata et al. 1986). Aluminum is found in 4-fold coordination in these materials, giving rise to chemical shifts in the range of  $+37$  to  $+44$  ppm relative to  $\text{Al}(\text{H}_2\text{O})_6^{3+}$ .

Blackwell and Patton (1984) report  $^{27}\text{Al}$  chemical shifts for 6-coordinate aluminum in metavariscite at  $-13.2$  ppm (MAS) and  $-12.4$  ppm (CP-MAS) relative to  $\text{Al}(\text{H}_2\text{O})_6^{3+}$ . These are probably not corrected for quadrupolar-induced shifts since other shifts tabulated in that paper were not. Since Blackwell and Patton (1984) did not provide the  $^{27}\text{Al}$  NMR spectra of metavariscite, we were unable to compute corrections. Incidentally, these two resonances cannot both arise from metavariscite since it contains only one crystallographically distinct aluminum per unit cell (Kniep and Mootz 1973). Müller et al. (1983a) found that 6-coordinate aluminum in calcium aluminum phosphate glasses resonate from  $-15$  ppm to  $-21$  ppm. The range is about the same for crystalline aluminum phosphates (Müller et al. 1983b). These shifts, and those for 4-coordinate aluminum, are about 30 ppm up-field relative to aluminas and aluminosilicates.

Alemaný et al. (1988) report, in the only published  $^{27}\text{Al}$  NMR study on 5-coordinate aluminum in aluminum phosphates, a chemical shift range of 14 ppm to 16 ppm. The up-field shift relative to 5-coordinate aluminum in oxides is 35 ppm to 45 ppm. Because so little is known about the chemical shift ranges for 5-coordinate aluminum in minerals, the estimates made by Alemaný et al. (1988) cannot be considered definitive.

We believe that the resonance in the  $^{27}\text{Al}$  NMR spectrum appearing at  $-8.9$  ppm in Fig. 1 is consistent with an assignment of aluminum to 6-fold coordination sites in taranakite even though it falls outside of the ranges mentioned above for that coordination number. We recognize the possible existence of aluminum in environments with quadrupolar coupling constants so large that an NMR signal is not observed under our experimental conditions. Acquisition of early portions of the FID, the length of the excitation pulse, the coordination number of the aluminum and the degree crystallinity of the material all greatly influence the probability that we will observe a signal in the  $^{27}\text{Al}$  NMR spectrum.

We used a spectral width of 125 kHz, corresponding to a "dead time" (the time during which the receiver is blanked after the excitation pulse and before FID acquisition begins) of 4  $\mu\text{s}$ . If we are missing a resonance, its full-width at half-height would have to be greater than 50 kHz

with a quadrupolar coupling constant greater than 12.5 MHz. Extending the spectral width, i.e. acquiring more of the initial portion of the FID, would not enhance resolution for such a broad resonance.

As mentioned in the section on methods and materials, we used an excitation-pulse of  $17^\circ$  (i.e. " $\pi/11$ " pulse). Since this is only slightly greater than the " $\pi/12$ " short-pulse limit (Samoson and Lippmaa 1983; Fenzke et al. 1984), the intensity of the resonance appearing in Fig. 1 is essentially independent of the quadrupolar-coupling-constants of any aluminum in the sample.

That taranakite is a crystalline compound is evidenced by the x-ray powder diffraction peaks we measured. Although crystallinity does not guarantee all of the aluminum will be observed, the body of evidence in the literature indicates that missing intensity is most often associated with poorly crystalline, amorphous or glassy material.

6-coordinate aluminum is consistently identified as being the coordination environment most likely to be unobserved. Andalusite is an excellent case in point (Alemany et al. 1986; Alemany et al. 1988). Here the central transition of 5-coordinate aluminum dominates the spectra while the signal arising from 6-coordinate aluminum is extremely difficult to resolve from the spinning side-bands. Contrariwise, the only resonance we observe in taranakite is the 6-coordinate aluminum. If there is a broad-line aluminum signal, experience suggests that it is most likely also to be 6-coordinate.

Taranakite belongs to the *hexagonal* crystal system. Observed x-ray reflections led Smith and Brown (1959) to assign taranakite to either space groups  $R3c$  or  $R\bar{3}c$ , both of which have three-fold axes along [0001]. On the basis of cell dimensions and chemical analyses, it is believed that the unit cell contains six layers and six formula units. The formula unit for taranakite is most commonly taken to be  $H_6K_3Al_5(PO_4)_8 \cdot nH_2O$  (Smith and Brown 1959). To be consistent with symmetry restrictions, three of the aluminum per layer should be related by the 3-fold axis and the other two lie on this axis. Hence, the ratio of aluminum chemical environments must be 2:3.

The cell dimensions and the symmetry of the taranakite crystals limit the number of distinct chemical environments possible within the unit cell. Pauling's "rule of parsimony" states that "the number of essentially different kinds of constituents in a crystal tends to be small" (Pauling 1929). These two arguments lead us to conclude that should there be some "undetected"  $^{27}Al$  in the taranakite structure, it must be on the order of 50% of the total aluminum in the sample. While it is true that NMR may reveal trace amounts of aluminum in other coordination environments, viz. the weak resonances at +55 ppm and +10 ppm (Fig. 1), it is unlikely these are significant components of the structure of taranakite. On the basis of the preceding discussion we conclude the aluminum in taranakite resides in exclusively six-fold coordination sites.

Crystal structure refinements for crandallite, (Blount 1974) variscite (Knipet et al. 1977) and wavellite (Araki and Zoltai 1968) reveal no direct protonation of phosphate oxygens occurs in these minerals. Potentially strong H-bonding interactions are found in crandallite (Blount 1974) where certain protons are disordered about an inversion center midway between the "O...O" contact in question. All of these cases follow the upper trace in Fig. 4, the weakly coupled group.

Monetite presents an interesting case in light of the results of the "interrupted decoupling" experiments. The magnetization-decay curve for this mineral (Fig. 4) clearly places it with the group of phosphates in which direct protonation of the phosphates is known not to occur. The protons associated with the phosphate oxygens in monetite appear to be disordered or shared in symmetrical hydrogen bonds (Dickens et al. 1972; Catti et al. 1977). The results of the "interrupted decoupling" experiment, however, suggest the protons in monetite cause  $^{31}P$  dephasing more like hydrogen-bonding protons than protons directly bonded to the phosphate oxygen.

There are two distinct phosphorus nuclear environments in taranakite. The phosphates represented by these two resonances clearly differ in their dipolar coupling with protons. The conclusion we draw from the "interrupted decoupling" experiments is that the -18.0 ppm resonance in taranakite involves a phosphate whose oxygens are, at most, hydrogen-bond receptors while the 4.5 ppm resonance arises from a phosphate with one or more oxygens are directly protonated. Dehydrating taranakite does not change the environments of the phosphorus since the dipolar dephasing dynamics of the two taranakites we studied are the same.

*Acknowledgements.* The authors are grateful to Steven R. Dec, who made the  $^{27}Al$  NMR measurements, and the Colorado State University Regional NMR Center, funded by National Science Foundation Grant No. CHE-8616437. The authors also acknowledge the help of Dr. Albert Rousseau (Centre d'Etudes Nucléaires de Grenoble) and Tom Boswell (Eastern Regional Research Center). W.F.B. wishes to thank Peter J. Dunn of the Department of Mineral Sciences, Natural Museum of Natural History-Smithsonian Institution, Washington, DC who generously provided the samples of taranakite, crandallite, variscite and wavellite and Ms. Amy Saunders who prepared the synthetic taranakite while a summer apprentice. Both authors are grateful to Professor P.H. Hsu of Rutgers University, New Brunswick, NJ for the x-ray powder diffraction analysis of the taranakite minerals used in this study.

## References

- Akitt JW, Farthing A (1978) New  $^{27}Al$  NMR studies of the hydrolysis of the aluminum(III) cation. *J Magn Reson* 32:345-352
- Akitt JW, Greenwood NN, Khandelwal BL, Lester GD (1972)  $^{27}Al$  nuclear magnetic resonance studies of the hydrolysis and polymerisation of the hexa-aquo-aluminum(III) cation. *J Chem Soc Dalton* 604-610
- Alemany LB, Kirker GW (1986) First observation of 5-coordinate aluminum by MAS  $^{27}Al$  NMR in well-characterized solids. *J Am Chem Soc* 108:6158-6162
- Alemany LB, Timken HKC, Johnson ID (1988) Aluminum-27 NMR study of  $AlPO_4$ -21 and andalusite. Advantages of high-field and very fast MAS. *J Magn Reson* 80:427-438
- Andrew ER (1981) Magic angle spinning. *Int Rev Phys Chem* 1:195-224
- Araki T, Zoltai T (1968) The crystal structure of wavellite. *Z Kristallogr* 127:21-33
- Aue WP, Roufosse AH, Glimcher MJ, Griffin RG (1984) Solid-state phosphorus-31 nuclear magnetic resonance studies of synthetic solid phases of calcium phosphate: Potential models of bone mineral. *Biochemistry* 23:6110-6114
- Blackwell CC, Patton RL (1984) Aluminum-27 and phosphorus-31 nuclear magnetic resonance studies of aluminophosphate molecular sieves. *J Phys Chem* 88:6135-6139
- Blount AM (1974) The crystal structure of crandallite. *Am Mineral* 59:41-47
- Boldog II, Golub AM, Kalinichenko AM (1979) Structure and

- thermal decomposition of taranakite and its analogues. *Russ J Inorg Chem (Engl Trans)* 21:190–194
- Bosacek V, Freude D, Fröhlich T, Pfeifer H, Schmiedel H (1982) NMR studies of  $^{27}\text{Al}$  in decationated Y zeolite. *J Colloid Interface Sci* 85:502–507
- Catti M, Ferraris G, Filhol A (1977) Hydrogen bonding in the crystalline state.  $\text{CaHPO}_4$  (monetite),  $\text{P1}$  or  $\text{P1}^-$ ? *Acta Crystallogr B33*:1223–1229
- Cheung TTP, Willcox KW, McDaniel MP, Johnson MM, Bronnemann C, Frye J (1986) The structure of coprecipitated aluminophosphate catalyst supports. *J Catal* 102:10–20
- Cruickshank DWJ, Robertson AP (1953) The comparison of theoretical and experimental determinations of molecular structures, with application to naphthalene and anthracene. *Acta Crystallogr* 6:698–705
- Cruickshank MC, Glasser LSD, Barri SAI, Poplett IJF (1986) Penta-co-ordinated aluminum: A solid-state  $^{27}\text{Al}$  NMR study. *J Chem Soc Chem Commun* 23–24
- De Jong BHWS, Schramm CM, Parziale VE (1983) Polymerization of silicate and aluminate tetrahedra in glasses, melts, and aqueous solutions – IV. Aluminum coordination in glasses and aqueous solutions and comments on the aluminum avoidance principle. *Geochim Cosmochim Acta* 47:1223–1236
- Dickens B, Bowen JS, Brown WE (1971) A refinement of the crystal structure of  $\text{CaHPO}_4$  (Synthetic monetite). *Acta Crystallogr B28*:797–806
- Dupree R, Holland D, Williams DS (1985) An examination by magic angle spinning NMR of the changes in the environment of  $^{27}\text{Al}$  during the devitrification of an aluminosilicate glass. *Phys Chem Glasses* 26:50–52
- Engelhardt G, Fahlke B, Mägi M, Lippmaa E (1983) High-resolution solid-state  $^{29}\text{Si}$  and  $^{27}\text{Al}$  NMR of aluminosilicate intermediates in zeolite A synthesis. *Zeolites* 3:292–294
- Fenzke D, Freude D, Fröhlich T, Haase J (1984) NMR intensity measurements of half-integer quadrupolar nuclei. *Chem Phys Lett* 111:171–175
- Freude D, Haase J, Klinowski J, Carpenter TA, Ronikier G (1985) NMR line shifts caused by the second-order quadrupolar interaction. *Chem Phys Lett* 119:365–367
- Fyfe CA, Beml L, Clark HC, Curtin D, Davies J, Drexler D, Dudley RL, Gobbi GC, Hartmen JS, Hayes P, Klinowski J, Lenkinski RE, Lock CJL, Paul IC, Rudin A, Tschir W, Thomas JM, Wasylischen FRS, Wasylischen RE (1982) Analytical chemical applications of high-resolution nuclear magnetic resonance spectroscopy of solids. *Philos Trans R Soc London Ser A* 305:591–607
- Fyfe CA, Beml L, Clark HC, Davies JA, Gobbi GC, Hartmen JS, Hayes PJ, Wasylischen RE (1983) High-resolution magic angle spinning and cross-polarization magic angle spinning solid-state NMR spectroscopy. In: Chisholm MH (ed) *Inorganic chemistry: toward the 21st century*. American Chemical Society, New York, pp 405–430
- Gilson JP, Edwards GC, Peters AW, Rajagopalan K, Wormsbecher RF, Roberie TG, Shatlock MP (1987) Penta-co-ordinated aluminum in zeolites and aluminosilicates. *J Chem Soc Chem Commun* 91–92
- Grimmer AR, Haubenreisser U (1983) High-field static and MAS  $^{31}\text{P}$  NMR: Chemical shift tensors of polycrystalline potassium phosphates  $\text{P}_2\text{O}_5 \cdot x\text{K}_2\text{O}$  ( $0 \leq x \leq 3$ ). *Chem Phys Lett* 99:487–490
- Grimmer AH, Starke P, Mägi M (1986) Charakterisierung von Kieselgelen durch die  $^1\text{H}$ - $^{29}\text{Si}$ -Kreuzpolarisations-Relaxationszeit  $T_{\text{SiH}}$  und die  $^1\text{H}$ -Spin-Gitter-Relaxationszeit  $T_{1\text{pH}}$ . *Z Chem* 26:114–115
- Haseman JF, Lehr JR, Smith JP (1950) Mineralogical character of some iron and aluminum phosphates containing potassium and ammonium. *Soil Sci Soc Am Proc* 15:76–84
- Herzfeld J, Berger AE (1980) Sideband intensities in NMR spectra of samples spinning at the magic angle. *J Chem Phys* 73:6021–6030
- Herzfeld J, Roufousse A, Haberkorn RA, Griffin RG, Glimcher MJ (1980) Magic angle sample spinning in inhomogeneously broadened biological systems. *Philos Trans R Soc London Ser B* 289:459–469
- Kirkpatrick RJ, Smith KA, Schramm S, Turner G, Yang WH (1985) Solid-state nuclear magnetic resonance spectroscopy of minerals. *Annu Rev Earth Planet Sci* 13:29–47
- Kirkpatrick RJ, Oestrike R, Weiss CA, Smith KA, Oldfield E (1986) High-resolution  $^{27}\text{Al}$  and  $^{29}\text{Si}$  NMR spectroscopy of glasses and crystals along the join  $\text{CaMgSi}_2\text{O}_6 - \text{CaAl}_2\text{SiO}_6$ . *Am Mineral* 71:705–711
- Klinowski J, Thomas JM, Fyfe CA, Gobbi GC (1982) Monitoring of structural changes accompanying ultrastabilization of faujasitic zeolite catalysts. *Nature* 296:533–536
- Kniep R, Mootz D (1973) Metavariscite – A redetermination of its crystal structure. *Acta Crystallogr B29*:2292–2294
- Kniep R, Mootz D, Vegas A (1977) Variscite. *Acta Crystallographica B33*:263–265
- Kundla E, Samoson A, Lippmaa E (1981) High-resolution NMR of quadrupolar nuclei in rotating solids. *Chem Phys Lett* 83:229–232
- Lampe VL, Müller D, Gessner W, Grimmer AR, Scheler G (1982) Vergleichende  $^{27}\text{Al}$ -NMR-Untersuchungen Am Mineral Zunit und basischen Aluminium-Salzen mit tridenameren Al-oxo-hydroxo-aquo-Kationen. *Z Anorg Allg Chem* 489:16–22
- Lippmaa E, Samoson A, Mägi M (1986) High resolution  $^{27}\text{Al}$  NMR of aluminosilicates. *J Am Chem Soc* 108:1730–1735
- Liu PL, Sherman GD, Swindale LD (1966) Laboratory formation and characterization of taranakite in a hydrol humic Latosol soil from Hawaii. *Pacific Sci* 20:496–506
- Maciel GE, Sindorf DW (1980) Silicon-29 nuclear magnetic resonance study of the surface of silica gel by cross polarization and magic-angle spinning. *J Am Chem Soc* 102:7606–7607
- Maricq MM, Waugh JS (1979) NMR in rotating solids. *J Chem Phys* 70:3300–3316
- Mastikhin VM, Zamaraev KI (1987) NMR studies of heterogeneous catalysis. *Z Phys Chem Munich* 152:59–80
- McConnell D (1976) Hypothetical phyllophosphate structure for taranakite. *Am Mineral* 61:329–331
- MacKenzie KJD, Brown IWM, Meinhold RH, Bowden ME (1985) Thermal reactions of pyrophyllite studied by high-resolution solid-state  $^{29}\text{Si}$  and  $^{27}\text{Al}$  nuclear magnetic resonance spectroscopy. *J Am Ceram Soc* 68:266–272
- Moore PB, Araki T (1979) Crystal structure of synthetic  $(\text{NH}_4)_3\text{H}_8\text{Fe}_3^{3+}(\text{PO}_4)_6 \cdot 6\text{H}_2\text{O}$ . *Am Mineral* 64:587–592
- Mudrakovskii IL, Mastikhin VM, Shmachkova VP, Kotsarenko NS (1985) High-resolution solid-state  $^{29}\text{Si}$  and  $^{31}\text{P}$  NMR of silicon-phosphorus compounds containing six-coordinated silicon. *Chem Phys Lett* 120:424–426
- Müller D, Jahn E, Fahlke B, Ladwig G, Haubenreisser U (1985) High resolution  $^{27}\text{Al}$  and  $^{31}\text{P}$  n.m.r. studies of the aluminum phosphate molecular sieve  $\text{AlPO}_4-5$ . *Zeolites* 5:53–56
- Müller D, Berger G, Grunze I, Ladwig G, Hallas E, Haubenreisser U (1983a) Solid-state high-resolution  $^{27}\text{Al}$  nuclear magnetic resonance studies of the structure of  $\text{CaO}-\text{Al}_2\text{O}_3-\text{P}_2\text{O}_5$  glasses. *Phys Chem Glasses* 24:37–42
- Müller D, Grunze I, Hallas E, Ladwig G (1983b) Hochfeld- $^{27}\text{Al}$ -NMR Untersuchungen zur Aluminiumkoordination in kristallinen Aluminiumphosphaten. *Z Anorg Allg Chem* 500:80–83
- Müller D, Gessner W, Behrens HJ, Scheler G (1981) Determination of the aluminum coordination in aluminum-oxygen compounds by solid-state high-resolution  $^{27}\text{Al}$  NMR. *Chem Phys Lett* 79:59–62
- Nagy JB, Engelhardt G, Michel D (1985) High resolution NMR on adsorbate-adsorbent systems. *Adv Colloid Interface Sci* 23:67–128
- Nakata SI, Asaoka S, Takahashi H, Deguchi K (1986) High-resolution solid-state phosphorus-31 MASNMR studies of inorganic phosphates. *Anal Sci* 2:91–93
- Nriagu JO (1984) Phosphate minerals: Their properties and general modes of occurrence. In: Nriagu JO, Moore PB (eds) *Phos-*

- phate minerals. Springer, Berlin Heidelberg New York, pp 1-136
- Oestrike R, Navrotsky A, Turner GL, Montez B, Kirkpatrick RJ (1987) Structural environment of Al dissolved in  $2\text{PbO} \cdot \text{B}_2\text{O}_3$  glasses used for solution colorimetry: An  $^{27}\text{Al}$  NMR study. *Am Mineral* 72:788-791
- Oldfield E, Kirkpatrick RJ (1985) High-resolution nuclear magnetic resonance of inorganic solids. *Science* 227:1537-1544
- Oldfield E, Kinsey RA, Smith KA, Nichols JA, Kirkpatrick RJ (1983) High-resolution NMR of inorganic solids. Influence of magnetic centers on magic-angle sample-spinning lineshapes in some natural aluminosilicates. *J Magn Reson* 51:325-329
- Opella SJ, Frey MH (1979) Selection of nonprotonated carbon resonances in solid-state nuclear magnetic resonance. *J Am Chem Soc* 101:5854-5856
- Pauling L (1929) The principles determining the structure of complex ionic crystals. *J Am Chem Soc* 51:1010-1027
- Pines A, Gibby MG, Waugh JS (1973) Proton-enhanced NMR of dilute spins in solids. *J Chem Phys* 59:569-590
- Resing HA, Rubinstein M (1978) Hydrolysis of crystalline aluminosilicate catalysts.  $^{27}\text{Al}$  NMR of hydrated zeolite 13-X. *J Colloid Interface Sci* 64:48-56
- Rothwell WP, Waugh JS, Yesinowski JP (1980) High-resolution variable-temperature  $^{31}\text{P}$  NMR of solid calcium phosphates. *J Am Chem Soc* 102:2637-2643
- Roufosse AH, Aue WP, Roberts JE, Glimche MJ, Griffin RG (1984) Investigations of the mineral phases of bone by solid-state phosphorus-31 magic angle spinning nuclear magnetic resonance. *Biochemistry* 23:6115-6120
- Sakae T, Sudo T (1975) Taranakite from the Onino-Iwaya limestone cave at Hiroshima Prefecture, Japan: A new occurrence. *Am Mineral* 60:331-334
- Samson A, Lippmaa E (1983) Excitation phenomena and line intensities in high-resolution NMR powder spectra of half-integer quadrupolar nuclei. *Phys Rev B* 28:6567-6570
- Sanz J, Serratos JM (1984) Distinction of tetrahedrally and octahedrally coordinated Al in phyllosilicates by NMR spectroscopy. *Clay Minerals* 19:113-115
- Smith JP, Brown WE (1959) X-ray studies of aluminum and iron phosphates containing potassium or ammonium. *Am Mineral* 44:138-142
- Stade H, Müller D, Scheler G (1984)  $^{27}\text{Al}$ -NMR-spektroskopische Untersuchungen zur Koordination des Al in C-S-H(Di, Poly). *Z Anorg Allg Chem* 510:16-24
- Taylor AW, Gurney EL (1961) Solubilities of potassium and ammonium taranakites. *J Phys Chem* 65:1613-1616
- Thompson AR, Kunwar AC, Gutowsky HS, Oldfield E (1987) Oxygen-17 and Aluminium-27 nuclear magnetic resonance spectroscopic investigations of aluminium(III) hydrolysis products. *J Chem Soc Dalton* 2317-2322
- Thong N, Schwarzenbach D (1979) The use of electric field gradient calculations in charge density refinements. II. Charge density refinement of the low-quartz structure of aluminum phosphate. *Acta Crystallogr A* 35:658-664
- Tropp J, Blumenthal NC, Waugh JS (1983) Phosphorus NMR study of solid amorphous calcium phosphate. *J Am Chem Soc* 105:22-26
- Turner GL, Smith KA, Kirkpatrick RJ, Oldfield E (1986) Structure and cation effects on phosphorus-31 NMR chemical shifts and chemical-shift anisotropies of orthophosphates. *J Magn Reson* 70:408-415